https://doi.org/10.5194/ar-2025-19
Preprint. Discussion started: 23 June 2025

A Cross-Correlation Based Method for Determining Size-Resolved Particle Growth Rates

Janne Lampilahti[1], Pauli Paasonen[1], Santeri Tuovinen[1], Katrianne Lehtipalo[1,2], Veli-Matti Kerminen[1], Markku Kulmala[1]

[1]Institute for Atmospheric and Earth System Research, University of Helsinki, Helsinki, Finland
[2]Finnish Meteorological Institute, Helsinki, Finland

Correspondence to: Janne Lampilahti (janne.lampilahti@helsinki.fi)

Abstract. The particle growth rate (GR) is a key parameter in aerosol dynamics and plays a crucial role in understanding atmospheric new particle formation and its effects. A fast, robust and reproducible calculation of GRs from aerosol number-size distribution data remains a challenge. In this study, we introduce a new method that we call the maximum correlation method for calculating particle and ion GRs from number-size distributions. We employed this novel method to calculate GRs from Hyytiälä, Finland using 14 years of ion and total particle size distribution data and compared our results against previous studies that used conventional methods for calculating the GRs. We found that our method compares well against the published data and reproduces the seasonal variability and size-dependent trends in the GRs. The maximum correlation method enables fast and repeatable GR calculations from large aerosol datasets, which facilitates the systematic incorporation of GR analysis into new particle formation studies.

1 Introduction

New particle formation (NPF) is the process by which gas-phase molecules cluster and grow to form stable aerosol particles in the atmosphere (e.g. Kulmala et al., 2013). NPF plays a critical role in the climate system, as it serves as a major source of cloud condensation nuclei (CCN), which influence cloud properties and radiative forcing in the atmosphere (Gordon et al., 2017; Merikanto et al., 2009; Yu and Luo, 2009; Zhao et al., 2024).

Particle growth rate (GR), defined as the rate of change of particle diameter, is a key quantity characterizing NPF (Kulmala et al., 2012). GR is an important parameter when determining the probability that the freshly formed particles reach CCN sizes, especially when the particles are only a few nanometers in diameter and easily scavenged by the pre-existing aerosol (Cai et al., 2022; e.g. Kerminen et al., 2018; Stolzenburg et al., 2018; Yli-Juuti et al., 2011).

https://doi.org/10.5194/ar-2025-19
Preprint. Discussion started: 23 June 2025

In ambient observations the GR is often determined from particle or ion concentration measurements that are resolved by both size and time. The methods to calculate GR can be roughly divided into two categories: number size distribution based methods and size channel based methods. In both methods one determines a so-called apparent GR, which represents the observed growth of the particle population at the measurement coordinates over the duration of the NPF event. The apparent GR does not separate out any processes responsible for the observed particle population growth (e.g. condensational growth, coagulation or size-dependent loss processes) and it does not determine GR of any single particle. A spatial homogeneity assumption is often made, which states that the apparent GR is equal to the average GR of the aerosol particle population.

In number size distribution based methods the GR is determined by analyzing the number size distribution across time. In the so-called mode fitting method (Dal Maso et al., 2005; Kulmala et al., 2012) a log-normal distribution is fitted to the growing particle mode at successive time steps and the rate of change of the peak values is used at calculating the GR. Usually a line is fitted through the peaks in a selected size range and the corresponding GR is reported as the slope of the fit. This method works best when the growing particle mode is fully visible in the data, instead of continuing to sizes smaller (or larger) than measured with the applied instrument. Paasonen et al. (2018) developed an automatic method based on mode fitting that identifies growing particle modes and calculates their GRs. However, the method is less reliable for determining GRs in the smallest particle sizes at the onset of NPF events.

In size channel based methods, the GR is determined by analysing the concentration time series across different size channels. A conventional approach is to fit a function to the increasing concentrations associated with the growing particle mode and track specific features from the fitted curves. In the maximum concentration method, a Gaussian function is used, and the peak positions determine the GR (Hirsikko et al., 2005). In the appearance time method, a sigmoid function is fitted to the leading edges of the rising concentrations, and the midpoint values are used to calculate the GR (Lehtipalo et al., 2014). This method is suitable also for cases when NPF is sustained over longer time periods, e.g. during chamber experiments (Dada et al., 2020), and therefore Gaussian function is not suitable for locating the maximum concentration.

A related approach is to estimate the time lag between the rising concentrations in two separate size channels (Riccobono et al., 2012; Sihto et al., 2006). The GR is calculated by dividing the size difference with the time lag. The size channel based methods are suitable for narrow size range instruments and when the particle mode is not fully visible in the data, which is usually the case when the growing particles are sub-5 nm in size.

In both number size distribution and size channel based methods automating the fitting procedure for NPF events is challenging. The range of data around the NPF event used for the fitting is usually manually selected by the researcher. This makes GR calculation labor-intensive and subjective. Additionally, fitting-based methods can be very sensitive to the chosen data range, leading to variability in GR estimates and reduced reproducibility. In part due to these limitations, despite the

https://doi.org/10.5194/ar-2025-19
Preprint. Discussion started: 23 June 2025

abundance of aerosol number-size distribution data, comprehensive datasets that report GRs in different size ranges are scarce.

In this study we introduce the maximum correlation method, which is an automatic time lag based method for GR calculation. Our objective is to apply this method to a large aerosol particle dataset collected from Hyytiälä, Finland, and compare the results with previously published size-resolved GR datasets from the same location.

2 Methods

2.1 Maximum correlation method

When no other processes significantly influence the particle size distribution, particle growth during or after an NPF event leads to an increase in particle number concentration that is observed earlier in the smaller size channels and later in the larger size channels. The task is to find a way to calculate the time displacement between the concentration rise for the different size channels and use it in the calculation of the GR.

We assume that a good condition for finding the optimal time displacement is when the concentrations in two size channels are maximally correlated. Next we will outline how this idea is used to calculate particle GRs from number-size distribution data.

1. Let us choose particle diameters d_1 and d_2 ($d_1 < d_2$) from the number size distribution
2. From the number-size distribution interpolate the concentration time series $N_1(t)$ and $N_2(t)$ that correspond to the size channels represented by the chosen diameters.
    a. It is possible to select an arbitrary time window for the time t. Here we chose one day from midnight to midnight local time since NPF tends to follow a diurnal cycle in most environments.
    b. Here we required that no more than 5% of the concentration values in the size range of interest were missing, otherwise the day was categorized as bad data. Days when the instrument was not measuring were also categorized as bad data.
3. Calculate normalized cross-correlation for $N_1(t)$ and $N_2(t)$:

$$R_{N_1N_2}(\tau) = \frac{1}{M(\tau)}\sum_{t} \frac{(N_1(t-\tau) - \underline{N_1})(N_2(t) - \underline{N_2})}{\sigma_1\sigma_2}$$

    a. $N_1(t)$ and $N_2(t)$ are normalized by subtracting their means $\underline{N_1}$ and $\underline{N_2}$ and dividing by their standard deviations σ_1 and σ_2. This makes the method less sensitive to baseline concentration levels or the differences in concentration amplitude.
    b. τ is the time displacement. Unless otherwise stated we varied τ from -23 h to 23 h at increments of 1s. We refer to the limiting displacement value as τ_{lim}.

https://doi.org/10.5194/ar-2025-19
Preprint. Discussion started: 23 June 2025

   c. $M(\tau)$ is the number of overlapping data points between time series $N_1(t)$ and $N_2(t)$ for a given τ. We divide the sum by $M(\tau)$ in order to reduce the effect of overlap on the cross-correlation since more overlapping points lead to a higher cross-correlation.
   d. In this study the channel concentrations $N_1(t)$ and $N_2(t)$ were smoothed using a 3 hour rolling mean. The concentration increases caused by regional NPF are expected to last several hours and the smoothing window width is optimized for preserving these peaks while removing higher frequency fluctuations that could cause erroneous values for the cross correlation. The chosen smoothing window width depends on the noise level of the data and time scale of the particle growth process under study.
4. Find the time displacement at maximum correlation $\tau_{max} = arg\ max(R_{N_1N_2}(\tau))$
   a. Return a missing value for results where $\tau_{max} \leq 0$s and for the limiting case $\tau_{max} = \tau_{lim}$
5. Calculate the growth rate as $GR_{d_1-d_2} = \frac{d_2 - d_1}{\tau_{max}}$

Figure 1 illustrates how the maximum correlation method is used to calculate particle GR from the number size distribution. In this case we calculated the GR of negative ions from 2 nm to 3 nm. The maximum concentration method was also applied to the case for comparison.

If the diameters d_1 and d_2 are too widely spaced, the correlation between the size channels is influenced by unrelated atmospheric processes. This is why the size range may have to be divided into smaller size increments and then the maximum correlation method can be applied to each smaller size range separately. In order to calculate GR for the whole size range one should add the maximum correlation time displacements $\tau_{max,i}$ for each smaller size range numbered by i

$$\tau_{max} = \sum_{i=1}^{n} \tau_{max,i}$$

and use the resulting τ_{max} in the final GR calculation. Here we used a condition that if for any of the smaller size ranges $\tau_{max,i} \leq 0$ or $\tau_{max,i} = \tau_{lim}$ then the GR for the whole size range would also be a missing value.

2.2 Hyytiälä dataset

The maximum correlation method can be used on individual days when a growing particle mode is present or to determine the distribution of GRs across multiple days in an automated fashion, as demonstrated in this study.

We tested the method on an ion and total particle number size distribution (INSD/PNSD) dataset from the SMEAR II station. SMEAR II station is located in Hyytiälä, Finland in a rural boreal forest environment (24.30E, 61.85N, 180m; Hari and Kulmala, 2005). The dataset is approximately 14 years long (Feb 2010-Dec 2024). No NPF event classification was done on the days in the dataset prior to the GR analysis. The INSDs and PNSDs were measured by a Neutral cluster and Air Ion

https://doi.org/10.5194/ar-2025-19
Preprint. Discussion started: 23 June 2025

Spectrometer (NAIS, Ariel Ltd.; Mirme and Mirme, 2013) and Differential Mobility Particle Sizer (DMPS; Aalto et al., 2001).

The NAIS measured the number size distribution of air ions and total particles in the mobility equivalent diameter range of approximately 0.8-40 nm and 2.5-40 nm respectively. The DMPS system measured the number size distribution of total particles in the mobility equivalent diameter range of 3-1000 nm. The number size distributions were averaged to 1 hour time resolution.

GRs were calculated in three size ranges: 2–3 nm, 3–7 nm and 7–20 nm. To ensure each size range was separately subdivided into smaller, equally spaced logarithmic bins: two bins for 2–3 nm, three for 3–7 nm, and four for 7–20 nm. The concentrations at each diameter were interpolated from the number size distribution (number concentrations normalized by logarithm of bin width, $dN/d\ log_{10}\ d$) measured by the NAIS or the DMPS.

We chose the above instruments and size ranges since comparable GR datasets already exist from Hyytiälä (Gonzalez Carracedo et al., 2022; Hirsikko et al., 2005; Manninen et al., 2009, 2010; Yli-Juuti et al., 2011).

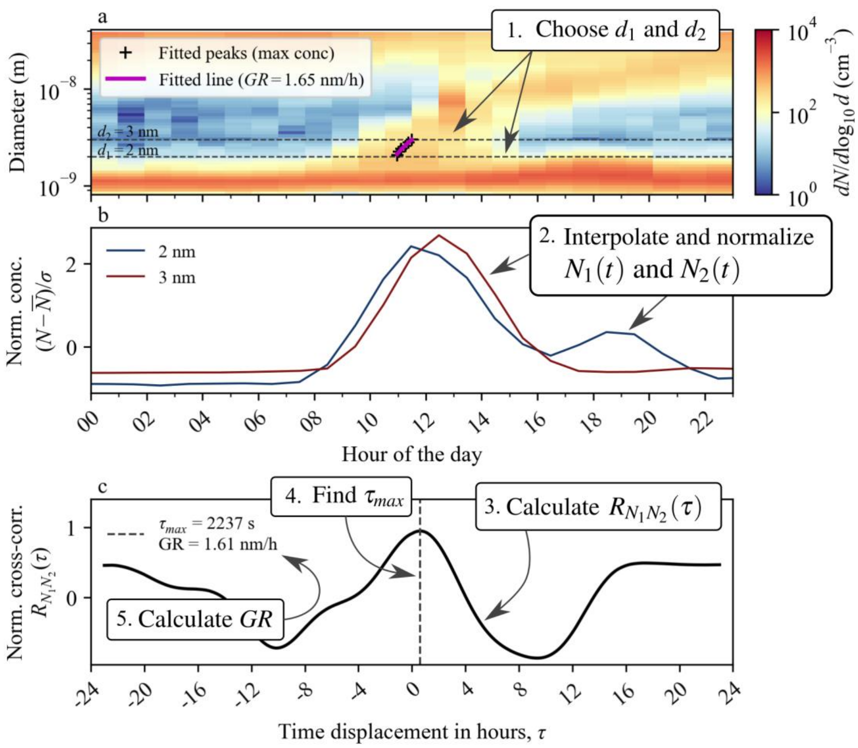

Figure 1: Example case from 15 March 2010 illustrating the calculation of GR for 2-3 nm negative ions using the maximum correlation method. (a) Negative INSD measured by the NAIS with peak diameters fitted using the maximum concentration method and the GR found by fitting a line to them, (b)

https://doi.org/10.5194/ar-2025-19
Preprint. Discussion started: 23 June 2025

normalized particle concentrations in the two size channels (rolling mean not applied yet), and (c) cross-correlation between size channels, with the maximum correlation and corresponding growth rate shown. For the purpose of illustrating the method the size range was not divided into smaller increments.

3 Results and discussion

The GR distributions obtained from the 14-year dataset in Hyytiälä using the maximum correlation method are shown in Figure 2. The distributions appear to consist of two distinct parts that we call the background and the signal.

We separated the signal distribution from the background by identifying a local minimum, β, between them. The likely reason for the background distribution at very low GRs is that the small number of overlapping points at large τ can produce relatively high cross-correlations, especially with the normalization. In the absence of particle growth the maximum cross correlation tends to occur when the early morning of the smaller size channel is aligned with the late evening of the larger size channel, leading to a distribution of low GR values.

To further illustrate this we prepared Figures A1-A6, which show examples of negative INSDs on days that are from the signal distribution and on days that are from the background distribution for each analyzed size class. The majority of the signal days, especially looking at the larger size ranges, show features typical of NPF days, while the background days contain mostly days that would be classified as non-event of undefined days (Dal Maso et al., 2005). This supports excluding them from the GR analysis.

The number of large outliers is relatively small in all GR distributions, which suggests that most local particle plumes that might cause very high GRs are filtered away by the requirement that $\tau_{max} > 0$s. We chose to ignore the large outliers due to their small number. In other environments the number of outliers may be higher due to increased local particle emissions.

As a result of separating out the background distribution, the remaining signal distribution contains the GR values from the days with true particle growth. If no signal distribution is visible it is likely because particle growth is not happening or not detected by the measurement. However, further testing needs to be done by using data from environments that have extremely slow (e.g. Arctic sites) or fast (e.g. some coastal sites) particle growth to see if a similar separation into background and growth distributions occurs.

The effect of dividing the 3-7 nm size range equally into n smaller increments of logarithmic width $\Delta\, log_{10}\, d$ is illustrated in Figure 3a. Dividing the size range into two smaller increments already dramatically improved the signal-to-noise ratio in the GR distribution. Further increasing the number of increments removed high GR days from the distribution. This is because if there are more smaller size ranges the probability of getting $\tau_{max,i} = 0$ s, especially on high GR days, is increased and in this case a missing value is returned for the whole GR. In order to maximize the signal-to-noise ratio and minimize the number of discarded high GR days, we aimed for a log difference of approximately 0.1 for the size increments when dividing the size range.

https://doi.org/10.5194/ar-2025-19
Preprint. Discussion started: 23 June 2025

The effect of using different time displacement ranges is shown in Figure 3b. The choice of τ_{lim} does not significantly influence the shape of the signal distribution, however using larger τ_{lim} slightly reduces the number of days in the signal distribution. This is likely because for larger τ range there are more chances to find a τ_{max} that results in a missing value. The background distribution is pushed towards the smaller GRs as τ_{lim} is increased, which is in line with the idea that when there is no particle growth the τ_{max} tends to occur with less overlapping data points. The shape of the background distribution does not significantly change until $\tau_{lim} = 23.8$ h at which point the number of days in the background distribution is increased. This is likely because higher cross correlations occur when the number of overlapping data points becomes very small. The local minimum between the background and the signal is not much affected by the choice of $\Delta\ log_{10}\ d$ or τ_{lim}.

In addition there were days when GR could not be calculated due to the data quality not being good enough (bad data) or due to $\tau_{max} \leq$ 0s (negative or infinite GR) or $\tau_{max} = \tau_{lim}$ (limiting case). The number of days in each category is shown in Figure 4. The relatively large number of bad data is explained by our rather strict criteria for usable data (<5% missing data in the size range of interest). Additionally, days when the instrument was not measuring were categorized as bad data. By comparison Yli-Juuti et al. (2011) was able to calculate $GR_{1.5-3}$ on 5%, GR_{3-7} on 4% and GR_{7-20} on 2% of all the days using the conventional methods, which are clearly lower percentages compared to our method.

We investigated how well the GRs calculated using the maximum correlation method compare with GRs calculated using the maximum concentration method. We randomly sampled 25 days from the 3-7 nm negative ion GRs and calculated the GR in the corresponding size range using the maximum concentration method. Figure 5 shows strong positive correlation between the two sets of GRs ($\rho =$ 0.9). The number size distributions on these days are shown in Figure A3.

https://doi.org/10.5194/ar-2025-19
Preprint. Discussion started: 23 June 2025

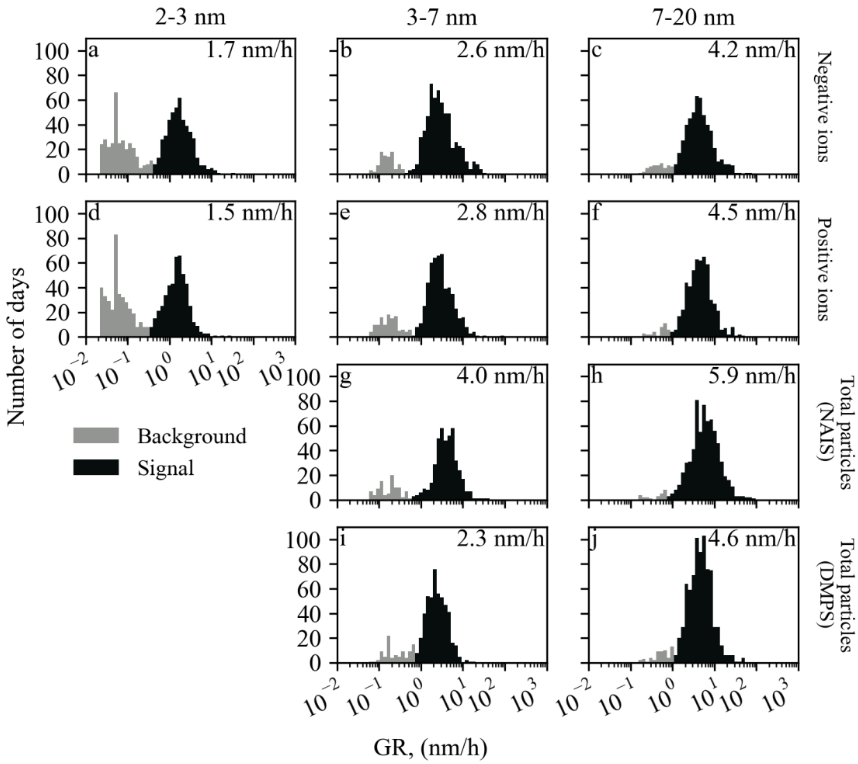

Figure 2: The GR distributions are separated into background and signal parts. The median GR from the signal distribution is shown in the upper right corner.

https://doi.org/10.5194/ar-2025-19
Preprint. Discussion started: 23 June 2025

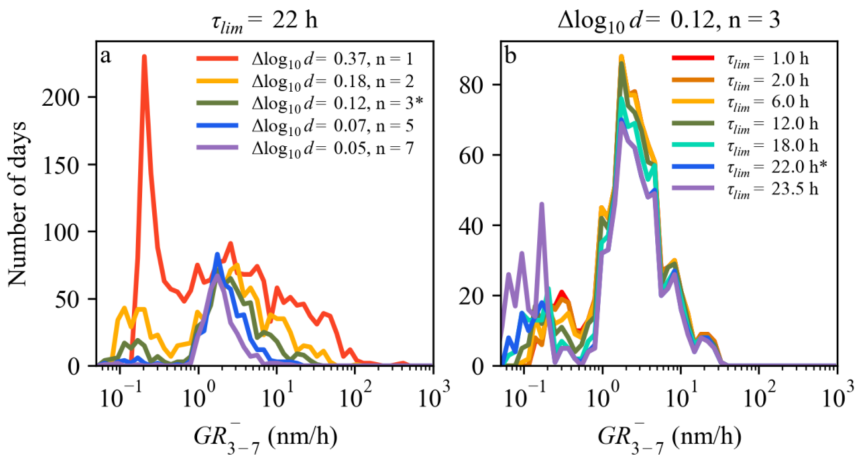

Figure 3: The effect of (a) dividing the size range into n smaller size increments of logarithmic width $\Delta \log_{10} d$ and (b) using different sized time displacement windows $\tau \in [-\tau_{lim}, \tau_{lim}]$. The GR distributions were calculated from negative ions. The values used in this study are marked with an asterisk.

https://doi.org/10.5194/ar-2025-19
Preprint. Discussion started: 23 June 2025

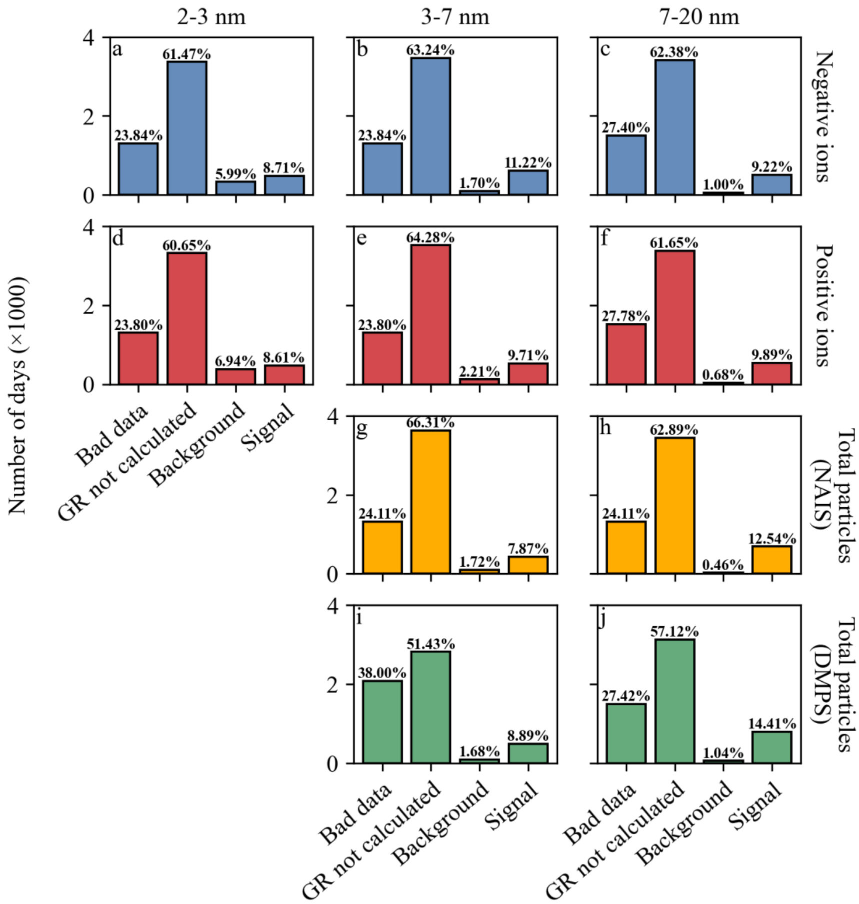

Figure 4: The number of days categorized as bad data, GR not calculated, background and signal. Percentage of total days is shown on top of each bar.

https://doi.org/10.5194/ar-2025-19
Preprint. Discussion started: 23 June 2025

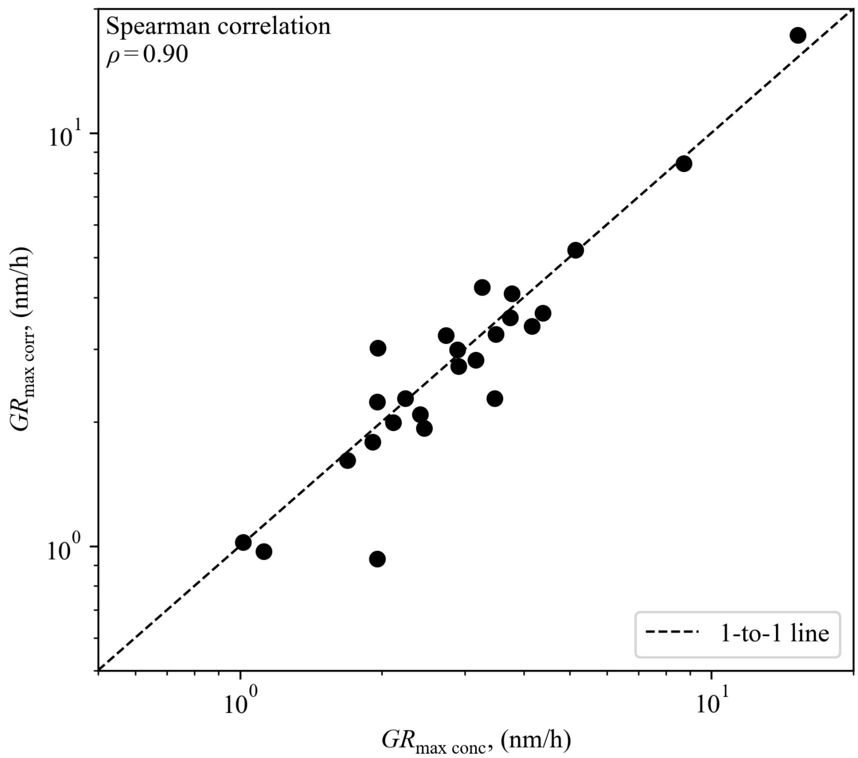

Figure 5: Comparison of GRs calculated using the maximum concentration and maximum correlation methods. The days were randomly selected from the 3-7 nm negative ion GRs. The number size distributions on these days are presented in Figure A3.

The median GRs showed an increasing trend with particle size, a pattern commonly observed across various environments (Kerminen et al., 2018). The median GRs found for the positive and negative ions are similar. This is also supported by previous observations, although in the smallest size range variation exists across studies (Gonzalez Carracedo et al., 2022; Hirsikko et al., 2005; Manninen et al., 2009; Yli-Juuti et al., 2011).

The median GRs calculated from the total particles measured by the NAIS are higher than the ones calculated from the ions, while the median GRs from DMPS agree better with the ion GRs. The other studies from Hyytiälä calculated the total particle GRs from DMPS or DMA-train data and found that they were overall similar to the ion GRs (Hirsikko et al., 2005; Manninen et al., 2009; Yli-Juuti et al., 2011), except in the sub-3 nm size range (Gonzalez Carracedo et al., 2022). This suggests that the GRs may be overestimated when calculated from the NAIS total particle mode.

Figure 6 illustrates the seasonal variation in the GRs. In 3-7 nm and 7-20 nm we observed a maximum in GRs during the summer months. Between 2-3 nm the ion GRs stay more constant

https://doi.org/10.5194/ar-2025-19
Preprint. Discussion started: 23 June 2025

throughout the year, although a summer maximum is seen in negative ions. This seasonal behavior of GRs is a common characteristic observed in Hyytiälä (Nieminen et al., 2018; Paasonen et al., 2018; Yli-Juuti et al., 2011)

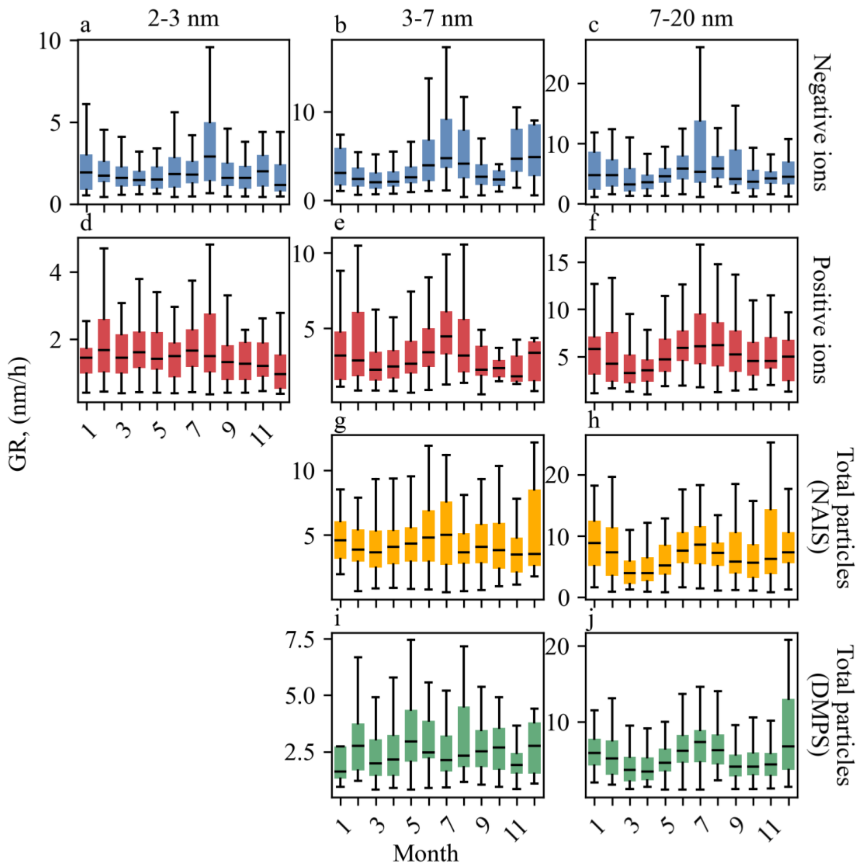

Figure 6: Seasonal variation of the GRs.

Next we divided the GR data in each size range into two parts: days where the GR was below the median (low GRs) and days where the GR was above or equal to the median (high GRs). Figure 7 shows the median diurnal cycles of the normalized negative INSDs for low and high GR days. Each diurnal cycle shows a growing negative ion mode that is first detected in the smallest sizes around midday. This is a defining feature of NPF. The slope of the growing ion mode in the size range of interest increases when going from low to high GRs.

https://doi.org/10.5194/ar-2025-19
Preprint. Discussion started: 23 June 2025

This shows that the GRs detected by our method are related to particle growth during NPF. Furthermore the data indicates that on low GR days the ions indeed grow slower compared to high GR days.

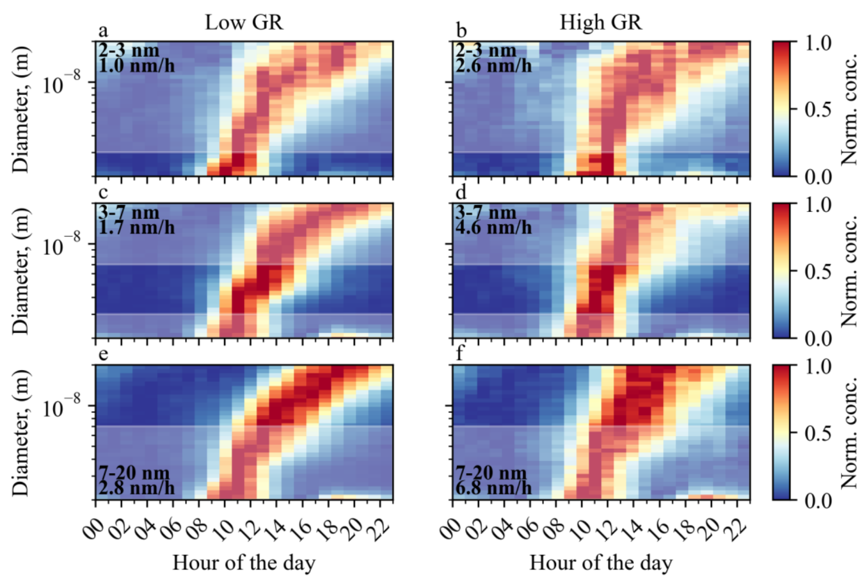

Figure 7: Median diurnal normalized negative INSDs in the different size ranges for low and high GRs. The size range where the GR was calculated is shown in each subplot and also indicated by the fully transparent area on the plot. The median GR is shown below the size ranges.

Finally, we compared our results with published GR data from Hyytiälä. Yli-Juuti et al. (2011) employed different instruments and methods to comprehensively study ion and total particle GRs during NPF events in Hyytiälä between 2003-2009. The instruments included an Air Ion Spectrometer (AIS, Mirme et al., 2007), which is an earlier version of the NAIS used in this study, a DMPS and a Balanced Scanning Mobility Analyzer (BSMA). The GRs were calculated from all the instruments using the maximum concentration method, while the mode fitting method was only used on the DMPS data. It should be noted that the correlation between the methods was found to be rather good (R=0.72), but the maximum concentration method typically showed slightly higher values (median difference 1.1 nm/h). For the smallest size range (1.5-3 nm) only ion data was used and for the larger size ranges (3-7 nm and 7-20 nm) both ion and total particle data were used. The reported final median GRs in each size class were averages of all the GRs calculated from the different instruments and methods (median GR was calculated from each method/instrument pair and mean was taken over the resulting median GRs).

Hirsikko et al. (2005) used data from the same instruments as Yli-Juuti et al. (2011) between 2003-2004, however only the maximum concentration method was used to calculate the GRs and the

https://doi.org/10.5194/ar-2025-19
Preprint. Discussion started: 23 June 2025

smallest size range was 1.3-3 nm. Otherwise the median GR was calculated similarly to Yli-Juuti et al. (2011). Manninen et al. (2009) and (2010) used the same methodology as Hirsikko et al. (2005) for March-June 2007 and March 2008-May 2009 respectively.

Gonzalez Carracedo et al. (2022) used the appearance time method and the maximum concentration method to calculate GRs in two different size ranges from ions measured by NAIS and total particles measured by DMA train. The authors found good agreement between the two methods. The data was measured in Hyytiälä between March-September 2020. We chose only the ion GRs to calculate the median GR in the smallest size range (1.8-3.2 nm) and both ion and total particle GRs to calculate the median GR in the larger size range (3.2-8 nm).

For comparing our results we calculated the median 2-3 nm GR from ions and the median 3-7 nm and 7-20 nm GRs using ion and DMPS data. We used the 0 and 99 percentile values as our min and max values. The results of the comparison are shown in Figure 8. Overall the median GRs in all the size ranges compare well across all studies. Also the min-max ranges and the interquartile ranges of the GRs (if reported) compare well across the studies.

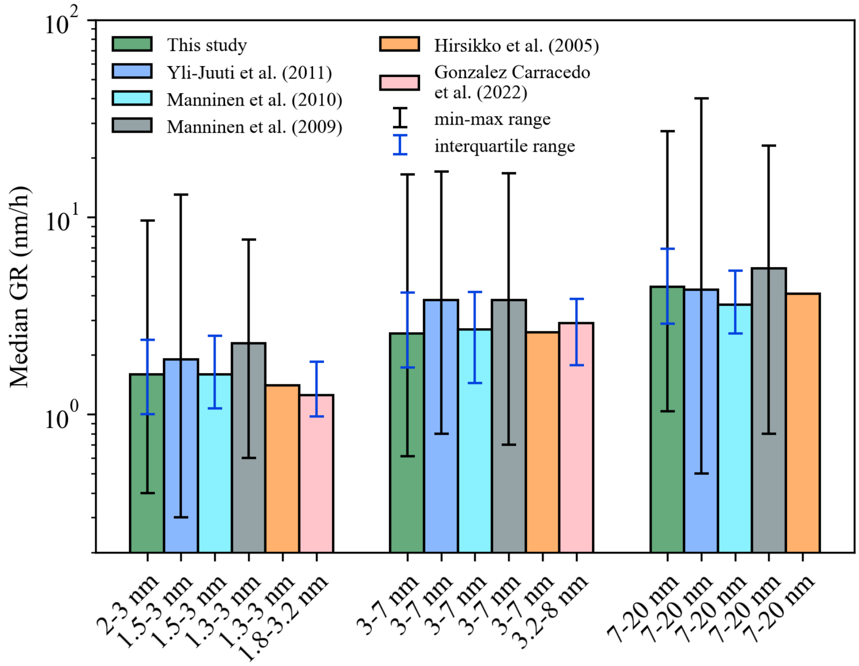

Figure 8: Comparison of GRs obtained in this study against published data from Hyytiälä. The bar height is the median GR in each size range and the error bars show different ranges of GR values reported in the studies.

https://doi.org/10.5194/ar-2025-19
Preprint. Discussion started: 23 June 2025

4 Conclusions

We presented a new method, called the maximum correlation method, for determining size-resolved particle GRs from aerosol number-size distribution data. The method was tested and validated in the sub-20 nm size range, showing its suitability for NPF studies. The proposed method is a time lag based method, which uses cross-correlation to determine the optimum time lag used for the GR calculation. We applied the method to approximately 14 years of ion and total particle data from the SMEAR II station in Hyytiälä, Finland and calculated GRs in three different size ranges: 2-3 nm, 3-7 nm and 7-20 nm.

The obtained median GRs, along with the variability measured by the interquartile range and the minimum–maximum range, were consistent with findings from previous studies. Our results reproduced the previously observed GR maximum during summer and an increasing GR as a function of particle size. On a subset of days, the GRs estimated by our method showed a positive correlation with those obtained using the maximum concentration method. Median diurnal negative INSDs on GR days and negative INSDs on example days showed that the growth of negative ions was predominantly due to NPF events.

One should keep in mind that the cross-correlation method gives the apparent GR of the particle population, which is roughly equal to the condensational GR under non-polluted environments with roughly homogenous sources of condensable vapors in surrounding areas. In polluted environments the effect of coagulation on the GR should be taken into account (Cai et al., 2021) and the heterogeneities in condensable vapor concentrations upwind the observation site alter strongly the apparent GR (Hakala et al., 2023; Kivekäs et al., 2016).

In the future it is important to test our method using aerosol data from other types of environments. For example in places with local emission sources there may be multiple particle growth events during a single day. In this case running the maximum correlation method using different time windows may be necessary in order to separate out the different growth processes. On the other hand, the suitability for detecting very low or very high GRs; as well as weak NPF should be further investigated.

The maximum correlation method allows one to efficiently and systematically calculate GRs from ion and total particle number size distributions. The proposed method is readily applied to large collections of data, which facilitates the GR analysis from new and existing aerosol datasets. When combined with statistical NPF classification methods, such as the nanoparticle ranking method (Aliaga et al., 2023), it could replace the conventional labor-intensive NPF analysis, especially when NPF is the dominant source of particles in the size range.

https://doi.org/10.5194/ar-2025-19
Preprint. Discussion started: 23 June 2025

343 **Appendix A**

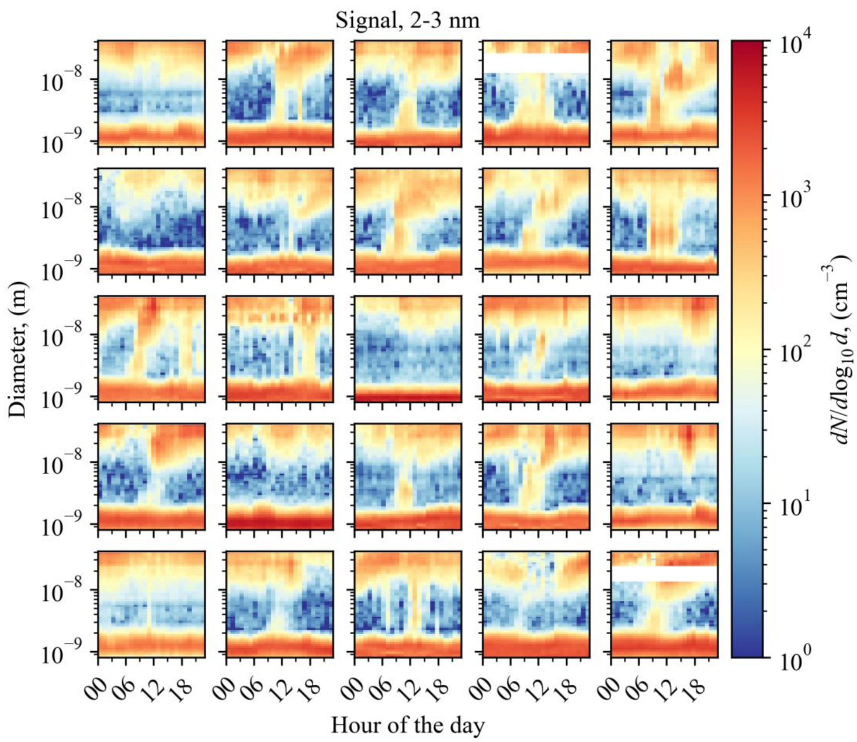

344
345 **Figure A1: Example negative INSDs on days sampled from the GR^{-}_{2-3} distribution's signal part.**

https://doi.org/10.5194/ar-2025-19
Preprint. Discussion started: 23 June 2025

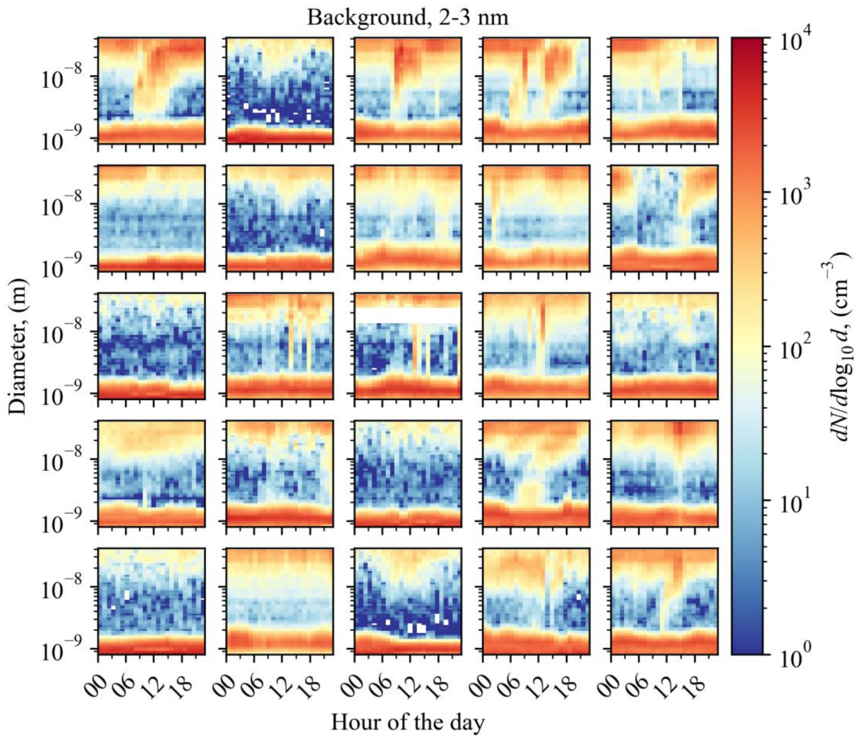

346
347 **Figure A2: Example negative INSDs on days sampled from the GR^{-}_{2-3} distribution's background part.**

https://doi.org/10.5194/ar-2025-19
Preprint. Discussion started: 23 June 2025

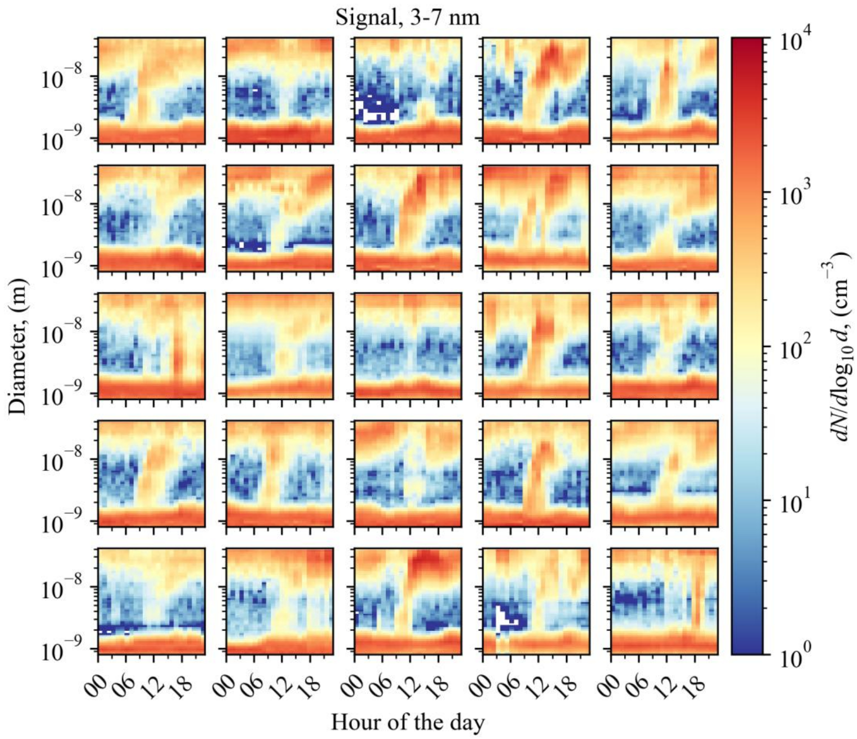

348
349 **Figure A3: Example negative INSDs on days sampled from the GR_{3-7}^{-} distribution's signal part.**

https://doi.org/10.5194/ar-2025-19
Preprint. Discussion started: 23 June 2025

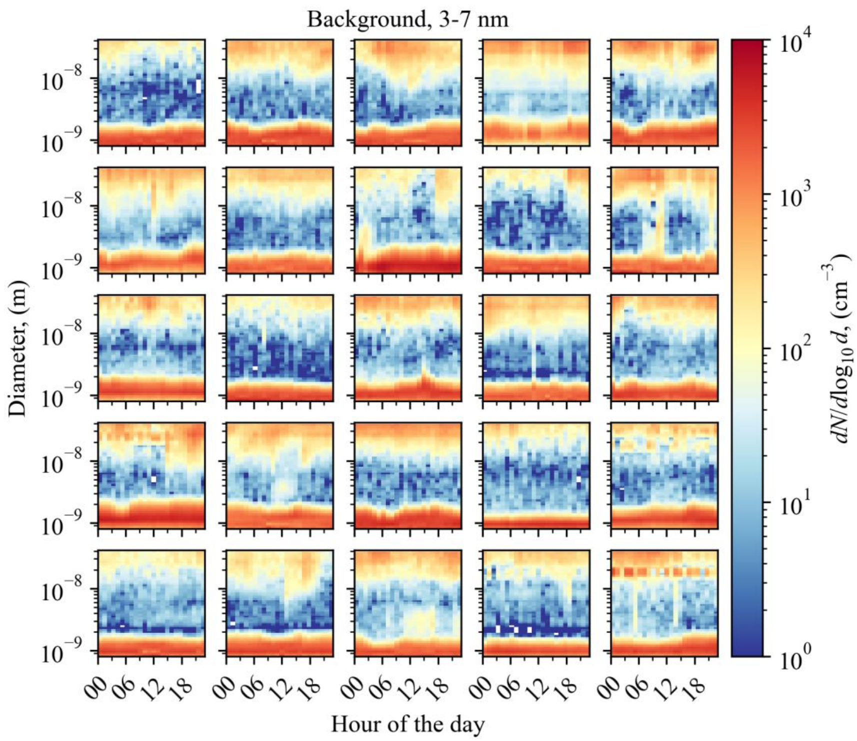

Figure A4: Example negative INSDs on days sampled from the GR^-_{3-7} distribution's background part.

https://doi.org/10.5194/ar-2025-19
Preprint. Discussion started: 23 June 2025

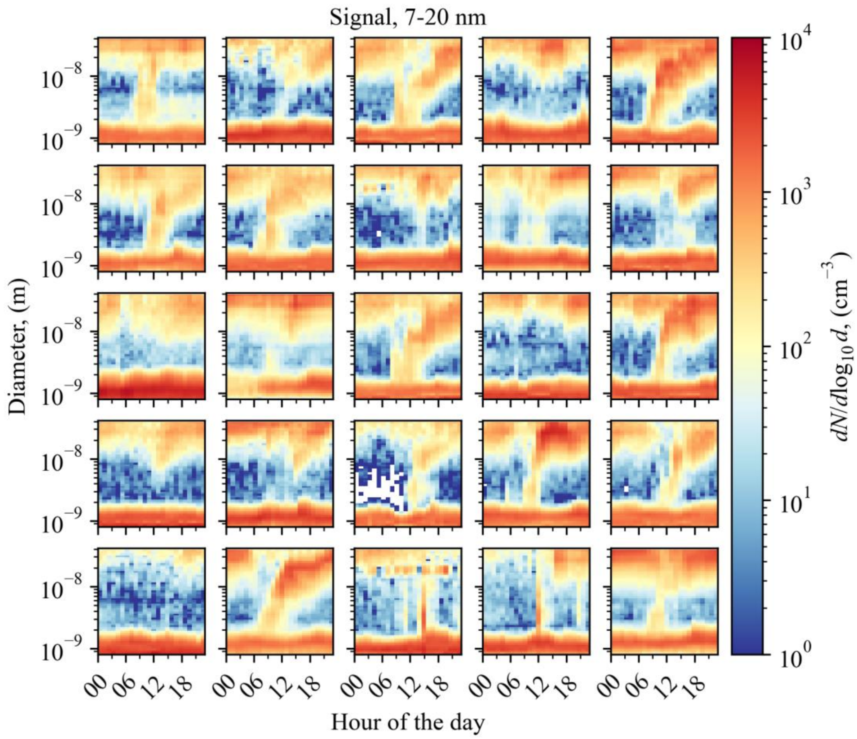

352
353 **Figure A5: Example negative INSDs on days sampled from the GR^{-}_{7-20} distribution's signal part.**

https://doi.org/10.5194/ar-2025-19
Preprint. Discussion started: 23 June 2025

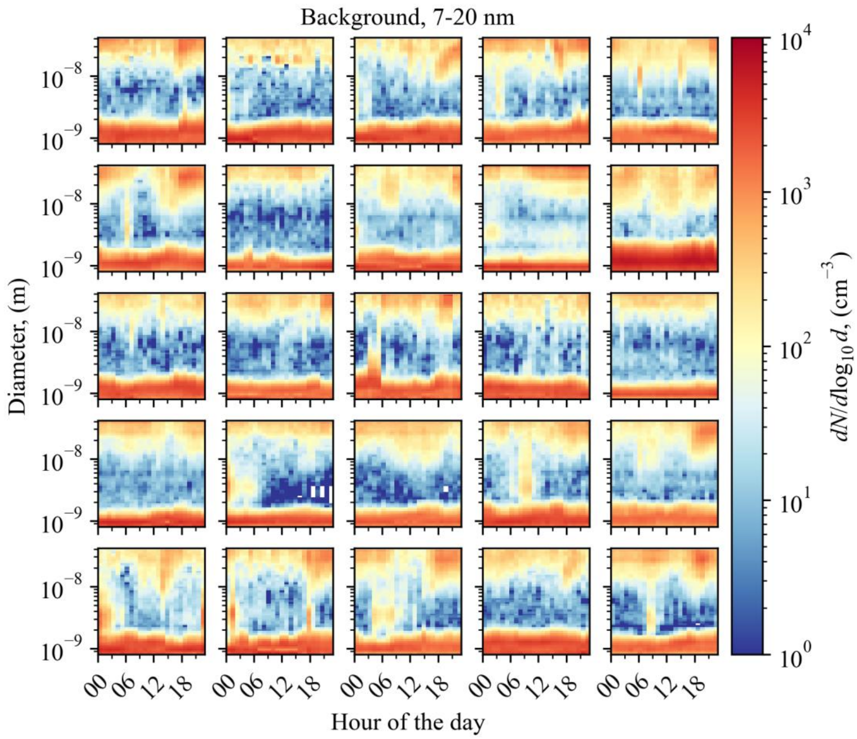

Figure A6: Example negative INSDs on days sampled from the GR^{-}_{7-20} distribution's background part.

Data availability. The NAIS dataset is available at https://doi.org/10.5281/zenodo.15648699 (Lampilahti et al., 2025). The DMPS dataset can be accessed through the SmartSMEAR data portal at https://smear.avaa.csc.fi/.

Author Contribution. JL conceived the method and conducted the data analysis. PP and MK contributed to refining the methodology. JL wrote the manuscript with input from all co-authors.

Competing interests. Some authors are members of the editorial board of Aerosol Research. The authors have no other competing interests to declare.

Acknowledgements. We acknowledge the University of Helsinki support via ACTRIS-HY. We acknowledge the staff at the SMEAR II field station for their valuable support in maintaining the measurement infrastructure and assisting with data collection.

Financial support. ACCC Flagship funded by the Academy of Finland grant number 337549 (UH), “Gigacity” project funded by Wihuri foundation, European Research Council (ERC) project ATM-

https://doi.org/10.5194/ar-2025-19
Preprint. Discussion started: 23 June 2025

GTP Contract No. 742206, Research Council of Finland University Profiling funding InterEarth (grant no. 353218), Research council of Finland project CO-ENHANCIN (project number 360114) and Horizon Europe project FOCI (project number 101056783).

References

Aalto, P., Hämeri, K., Becker, E., Weber, R., Salm, J., Mäkelä, J. M., Hoell, C., O'Dowd, C. D., Hansson, H.-C., Väkevä, M., Koponen, I. K., Buzorius, G., and Kulmala, M.: Physical characterization of aerosol particles during nucleation events, Tellus B, 53, 344–358, https://doi.org/10.3402/tellusb.v53i4.17127, 2001.

Aliaga, D., Tuovinen, S., Zhang, T., Lampilahti, J., Li, X., Ahonen, L., Kokkonen, T., Nieminen, T., Hakala, S., Paasonen, P., Bianchi, F., Worsnop, D., Kerminen, V.-M., and Kulmala, M.: Nanoparticle ranking analysis: determining new particle formation (NPF) event occurrence and intensity based on the concentration spectrum of formed (sub-5 nm) particles, Aerosol Research, 1, 81–92, https://doi.org/10.5194/ar-1-81-2023, 2023.

Cai, R., Li, C., He, X.-C., Deng, C., Lu, Y., Yin, R., Yan, C., Wang, L., Jiang, J., Kulmala, M., and Kangasluoma, J.: Impacts of coagulation on the appearance time method for new particle growth rate evaluation and their corrections, Atmospheric Chemistry and Physics, 21, 2287–2304, https://doi.org/10.5194/acp-21-2287-2021, 2021.

Cai, R., Deng, C., Stolzenburg, D., Li, C., Guo, J., Kerminen, V.-M., Jiang, J., Kulmala, M., and Kangasluoma, J.: Survival probability of new atmospheric particles: closure between theory and measurements from 1.4 to 100 nm, Atmospheric Chemistry and Physics, 22, 14571–14587, https://doi.org/10.5194/acp-22-14571-2022, 2022.

Dada, L., Lehtipalo, K., Kontkanen, J., Nieminen, T., Baalbaki, R., Ahonen, L., Duplissy, J., Yan, C., Chu, B., Petäjä, T., Lehtinen, K., Kerminen, V.-M., Kulmala, M., and Kangasluoma, J.: Formation and growth of sub-3-nm aerosol particles in experimental chambers, Nat Protoc, 15, 1013–1040, https://doi.org/10.1038/s41596-019-0274-z, 2020.

Dal Maso, M., Kulmala, M., Riipinen, I., Wagner, R., Hussein, T., Aalto, P. P., and Lehtinen, K. E.: Formation and growth of fresh atmospheric aerosols: eight years of aerosol size distribution data from SMEAR II, Hyytiälä, Finland, Boreal Environ. Res., 10, 323, 2005.

Gonzalez Carracedo, L., Lehtipalo, K., Ahonen, L. R., Sarnela, N., Holm, S., Kangasluoma, J., Kulmala, M., Winkler, P. M., and Stolzenburg, D.: On the relation between apparent ion and total particle growth rates in the boreal forest and related chamber experiments, Atmospheric Chemistry and Physics, 22, 13153–13166, https://doi.org/10.5194/acp-22-13153-2022, 2022.

Gordon, H., Kirkby, J., Baltensperger, U., Bianchi, F., Breitenlechner, M., Curtius, J., Dias, A., Dommen, J., Donahue, N. M., Dunne, E. M., Duplissy, J., Ehrhart, S., Flagan, R. C., Frege, C., Fuchs, C., Hansel, A., Hoyle, C. R., Kulmala, M., Kürten, A., Lehtipalo, K., Makhmutov, V., Molteni, U., Rissanen, M. P., Stozkhov, Y., Tröstl, J., Tsagkogeorgas, G., Wagner, R., Williamson, C., Wimmer, D., Winkler, P. M., Yan, C., and Carslaw, K. S.: Causes and importance of new particle formation in the present-day and preindustrial atmospheres, Journal of Geophysical Research: Atmospheres, 122, 8739–8760, https://doi.org/10.1002/2017JD026844, 2017.

Hakala, S., Vakkari, V., Lihavainen, H., Hyvärinen, A.-P., Neitola, K., Kontkanen, J., Kerminen, V.-M., Kulmala, M., Petäjä, T., Hussein, T., Khoder, M. I., Alghamdi, M. A., and Paasonen, P.: Explaining apparent particle shrinkage related to new particle formation events in western Saudi Arabia does not require evaporation, Atmospheric Chemistry and Physics, 23, 9287–9321, https://doi.org/10.5194/acp-23-9287-2023, 2023.

Hari, P. and Kulmala, M.: Station for measuring ecosystem-atmosphere relations (SMEAR II), Boreal Environ. Res., 10, 315–322, 2005.

Hirsikko, A., Laakso, L., Hõrrak, U., Aalto, P. P., Kerminen, V.-M., and Kulmala, M.: Annual and size dependent variation of growth rates and ion concentrations in boreal forest, Boreal Env. Res., 10, 357–369, 2005.

Kerminen, V.-M., Chen, X., Vakkari, V., Petäjä, T., Kulmala, M., and Bianchi, F.: Atmospheric new particle formation and growth: review of field observations, Environ. Res. Lett., 13, 103003, https://doi.org/10.1088/1748-9326/aadf3c, 2018.

Kivekäs, N., Carpman ,Jimmie, Roldin ,Pontus, Leppä ,Johannes, O'Connor ,Ewan, Kristensson ,Adam, and and Asmi, E.: Coupling an aerosol box model with one-dimensional flow: a tool for understanding observations of new particle formation events, Tellus B: Chemical and Physical Meteorology, 68, 29706, https://doi.org/10.3402/tellusb.v68.29706, 2016.

Kulmala, M., Petäjä, T., Nieminen, T., Sipilä, M., Manninen, H. E., Lehtipalo, K., Dal Maso, M., Aalto, P. P., Junninen, H., Paasonen, P., Riipinen, I., Lehtinen, K. E. J., Laaksonen, A., and Kerminen, V.-M.: Measurement of the nucleation of atmospheric aerosol particles, Nat. Protocols, 7, 1651–1667, https://doi.org/10.1038/nprot.2012.091, 2012.

Kulmala, M., Kontkanen, J., Junninen, H., Lehtipalo, K., Manninen, H. E., Nieminen, T., Petäjä, T., Sipilä, M., Schobesberger, S., Rantala, P., Franchin, A., Jokinen, T., Järvinen, E., Äijälä, M., Kangasluoma, J., Hakala, J., Aalto, P. P., Paasonen, P., Mikkilä, J., Vanhanen, J., Aalto, J., Hakola, H., Makkonen, U., Ruuskanen, T., Mauldin, R. L., Duplissy, J., Vehkamäki, H., Back, J., Kortelainen, A., Riipinen, I., Kurten, T., Johnston, M. V., Smith, J. N., Ehn, M., Mentel, T. F., Lehtinen, K. E. J., Laaksonen, A., Kerminen, V.-M., and Worsnop, D. R.: Direct observations of

https://doi.org/10.5194/ar-2025-19
Preprint. Discussion started: 23 June 2025

atmospheric aerosol nucleation, Science, 339, 943–946, https://doi.org/10.1126/science.1227385, 2013.

Lampilahti, J., Paasonen, P., Tuovinen, S., Lehtipalo, K., Kerminen, V.-M., and Kulmala, M.: Dataset for "A Cross-Correlation-Based Method for Determining Size-Resolved Particle Growth Rates," https://doi.org/10.5281/zenodo.15648699, 2025.

Lehtipalo, K., Leppä, J., Kontkanen, J., Kangasluoma, J., Franchin, A., Wimmer, D., Schobesberger, S., Junninen, H., Petäjä, T., Sipilä, M., Mikkilä, J., Vanhanen, J., Worsnop, D. R., and Kulmala, M.: Methods for determining particle size distribution and growth rates between 1 and 3 nm using the Particle Size Magnifier, Boreal Environ. Res., 19, 22, 2014.

Manninen, H. E., Nieminen, T., Riipinen, I., Yli-Juuti, T., Gagné, S., Asmi, E., Aalto, P. P., Petäjä, T., Kerminen, V.-M., and Kulmala, M.: Charged and total particle formation and growth rates during EUCAARI 2007 campaign in Hyytiälä, Atmos. Chem. Phys., 9, 4077–4089, https://doi.org/10.5194/acp-9-4077-2009, 2009.

Manninen, H. E., Nieminen, T., Asmi, E., Gagné, S., Häkkinen, S., Lehtipalo, K., Aalto, P., Vana, M., Mirme, A., Mirme, S., Hõrrak, U., Plass-Dülmer, C., Stange, G., Kiss, G., Hoffer, A., Törő, N., Moerman, M., Henzing, B., de Leeuw, G., Brinkenberg, M., Kouvarakis, G. N., Bougiatioti, A., Mihalopoulos, N., O'Dowd, C., Ceburnis, D., Arneth, A., Svenningsson, B., Swietlicki, E., Tarozzi, L., Decesari, S., Facchini, M. C., Birmili, W., Sonntag, A., Wiedensohler, A., Boulon, J., Sellegri, K., Laj, P., Gysel, M., Bukowiecki, N., Weingartner, E., Wehrle, G., Laaksonen, A., Hamed, A., Joutsensaari, J., Petäjä, T., Kerminen, V.-M., and Kulmala, M.: EUCAARI ion spectrometer measurements at 12 European sites – analysis of new particle formation events, Atmos. Chem. Phys., 10, 7907–7927, https://doi.org/10.5194/acp-10-7907-2010, 2010.

Merikanto, J., Spracklen, D. V., Mann, G. W., Pickering, S. J., and Carslaw, K. S.: Impact of nucleation on global CCN, Atmos. Chem. Phys., 9, 8601–8616, 2009.

Mirme, A., Tamm, E., Mordas, G., Vana, M., Uin, J., Mirme, S., Bernotas, T., Laakso, L., Hirsikko, A., and Kulmala, M.: A wide-range multi-channel Air Ion Spectrometer, Boreal Environ. Res., 12, 247–264, 2007.

Mirme, S. and Mirme, A.: The mathematical principles and design of the NAIS – a spectrometer for the measurement of cluster ion and nanometer aerosol size distributions, Atmos. Meas. Tech., 6, 1061–1071, https://doi.org/10.5194/amt-6-1061-2013, 2013.

Nieminen, T., Kerminen, V.-M., Petäjä, T., Aalto, P. P., Arshinov, M., Asmi, E., Baltensperger, U., Beddows, D. C. S., Beukes, J. P., Collins, D., Ding, A., Harrison, R. M., Henzing, B., Hooda, R., Hu, M., Hõrrak, U., Kivekäs, N., Komsaare, K., Krejci, R., Kristensson, A., Laakso, L., Laaksonen, A., Leaitch, W. R., Lihavainen, H., Mihalopoulos, N., Németh, Z., Nie, W., O'Dowd, C., Salma, I., Sellegri, K., Svenningsson, B., Swietlicki, E., Tunved, P., Ulevicius, V., Vakkari, V., Vana, M., Wiedensohler, A., Wu, Z., Virtanen, A., and Kulmala, M.: Global analysis of continental boundary layer new particle formation based on long-term measurements, Atmospheric Chemistry and Physics, 18, 14737–14756, https://doi.org/10.5194/acp-18-14737-2018, 2018.

Paasonen, P., Peltola, M., Kontkanen, J., Junninen, H., Kerminen, V.-M., and Kulmala, M.: Comprehensive analysis of particle growth rates from nucleation mode to cloud condensation nuclei in boreal forest, Atmospheric Chemistry and Physics, 18, 12085–12103, https://doi.org/10.5194/acp-18-12085-2018, 2018.

Riccobono, F., Rondo, L., Sipilä, M., Barmet, P., Curtius, J., Dommen, J., Ehn, M., Ehrhart, S., Kulmala, M., Kürten, A., Mikkilä, J., Paasonen, P., Petäjä, T., Weingartner, E., and Baltensperger, U.: Contribution of sulfuric acid and oxidized organic compounds to particle formation and growth, Atmospheric Chemistry and Physics, 12, 9427–9439, https://doi.org/10.5194/acp-12-9427-2012, 2012.

Sihto, S.-L., Kulmala, M., Kerminen, V.-M., Dal Maso, M., Petäjä, T., Riipinen, I., Korhonen, H., Arnold, F., Janson, R., Boy, M., Laaksonen, A., and Lehtinen, K. E. J.: Atmospheric sulphuric acid and aerosol formation: implications from atmospheric measurements for nucleation and early growth mechanisms, Atmospheric Chemistry and Physics, 6, 4079–4091, https://doi.org/10.5194/acp-6-4079-2006, 2006.

Stolzenburg, D., Fischer, L., Vogel, A. L., Heinritzi, M., Schervish, M., Simon, M., Wagner, A. C., Dada, L., Ahonen, L. R., Amorim, A., Baccarini, A., Bauer, P. S., Baumgartner, B., Bergen, A., Bianchi, F., Breitenlechner, M., Brilke, S., Mazon, S. B., Chen, D., Dias, A., Draper, D. C., Duplissy, J., Haddad, I. E., Finkenzeller, H., Frege, C., Fuchs, C., Garmash, O., Gordon, H., He, X., Helm, J., Hofbauer, V., Hoyle, C. R., Kim, C., Kirkby, J., Kontkanen, J., Kürten, A., Lampilahti, J., Lawler, M., Lehtipalo, K., Leiminger, M., Mai, H., Mathot, S., Mentler, B., Molteni, U., Nie, W., Nieminen, T., Nowak, J. B., Ojdanic, A., Onnela, A., Passananti, M., Petäjä, T., Quéléver, L. L. J., Rissanen, M. P., Sarnela, N., Schallhart, S., Tauber, C., Tomé, A., Wagner, R., Wang, M., Weitz, L., Wimmer, D., Xiao, M., Yan, C., Ye, P., Zha, Q., Baltensperger, U., Curtius, J., Dommen, J., Flagan, R. C., Kulmala, M., Smith, J. N., Worsnop, D. R., Hansel, A., Donahue, N. M., and Winkler, P. M.: Rapid growth of organic aerosol nanoparticles over a wide tropospheric temperature range, PNAS, 115, 9122–9127, https://doi.org/10.1073/pnas.1807604115, 2018.

Yli-Juuti, T., Nieminen, T., Hirsikko, A., Aalto, P. P., Asmi, E., Hõrrak, U., Manninen, H. E., Patokoski, J., Dal Maso, M., Petäjä, T., Rinne, J., Kulmala, M., and Riipinen, I.: Growth rates of nucleation mode particles in Hyytiälä during 2003-2009: variation with particle size, season, data analysis method and ambient conditions, Atmos. Chem. Phys., 11, 12865–12886, https://doi.org/10.5194/acp-11-12865-2011, 2011.

https://doi.org/10.5194/ar-2025-19
Preprint. Discussion started: 23 June 2025

Yu, F. and Luo, G.: Simulation of particle size distribution with a global aerosol model: contribution of nucleation to aerosol and CCN number concentrations, Atmos. Chem. Phys., 9, 7691–7710, 2009.

Zhao, B., Donahue, N. M., Zhang, K., Mao, L., Shrivastava, M., Ma, P.-L., Shen, J., Wang, S., Sun, J., Gordon, H., Tang, S., Fast, J., Wang, M., Gao, Y., Yan, C., Singh, B., Li, Z., Huang, L., Lou, S., Lin, G., Wang, H., Jiang, J., Ding, A., Nie, W., Qi, X., Chi, X., and Wang, L.: Global variability in atmospheric new particle formation mechanisms, Nature, 631, 98–105, https://doi.org/10.1038/s41586-024-07547-1, 2024.